

# Reconfigurable metamaterial for 5G application

M. M. HASAN<sup>a</sup>, E. AHAMED<sup>a</sup>, M. R. I. FARUQUE<sup>a</sup>, M. T. ISLAM<sup>b</sup>, S. ABDULLAH<sup>a</sup>

<sup>a</sup>Space Science Centre (ANGKASA), Universiti Kebangsaan Malaysia, Bangi 43600, Malaysia

<sup>b</sup>Center of Advanced Electronics and Communication Engineering, Universiti Kebangsaan Malaysia, Bangi 43600, Malaysia

A reconfigurable metamaterial for 5G application has been presented in this paper. The proposed structure is designed by the resonator with splits and an I-shape inner metal bar is connected with the ring resonator printed on an epoxy resin fiber material. A finite integration technique based electromagnetic simulator CST Microwave Studio has been used to design, simulation, and analysis purposes. The designed metamaterial exhibits resonance peaks at, 33.21, 39.89, 42.27, 45.86, and 48.41 GHz, respectively. Finally, the performances of the effective medium parameters at different switching state have been discussed for understanding the reconfigurable characteristics of the designed metamaterial.

(Received August 1, 2017; accepted August 9, 2018)

**Keywords:** Bandwidth, Effective Parameters, Reconfigurable Metamaterial

## 1. Introduction

The fifth generation (5G) networks are expected to use the higher frequency bandwidths due to the growing need for wider bandwidths and higher data rates. Compared with the cellular networks used today, 5G mobile networks will the proposed bands in the millimeter wave region are, 37.0 to 40.50 GHz, 42.50 to 43.50 GHz, 45.50 to 47.0 GHz, 47.20 to 50.20 GHz, which have allocations to the mobile service on a primary basis. Besides, 31.80 to 33.40 GHz, 40.50 to 42.50 GHz, and 47.0 to 47.20 GHz, which may require additional allocations to the mobile service on a primary basis for 5G wireless communications. Metamaterial is a term for an engineered artificial material, which consists of composite structure to exhibit the unique properties or characteristic of material not found in nature. At present, electronic devices are affordable to most of the persons and become an important gadget in their daily life. As a result, miniaturizations of electronic devices have great importance, especially in order to develop light-weight portable devices. The unique behaviors of metamaterials such as control the amplitude, phase, polarization and propagation direction of electromagnetic waves can be engineered through the design of structural geometry. In addition, the bandwidth, gain and efficiency of the antenna can be improved by embedding the metamaterial with the antenna for 5G application. In 2000, Smith et al. suggested a metamaterial that can be shown simultaneously negative permittivity and permeability. Besides, he did the microwave examinations to examine the proposed materials unusual properties [1]. A  $10 \times 10 \text{ mm}^2$  double negative metamaterial was presented for dual band (C- and X-) operations, which bandwidth was 3.60 GHz and the effective medium ratio was 4.0, where the operating frequencies were from 2.0 to 14.0 GHz [2]. In addition, a negative index metamaterial with two components analysis

for C- and X-band had been introduced by Islam et al. and the structure had two arrows and a metal arm was connected the two arrows that looked like a double arrow shape printed on the epoxy resin fiber and the epoxy resin formation processes were also explained step by step in 2017 [3]. A reconfigurable MMs was designed that not only had a wide tuning range of the resonance frequency up to 31% and 22% for the TE and the TM polarization, but also produced a high quality factor resonance [4]. A digital MMs with selectively reconfigurable micro-cantilevers integrated into a single unit cell for control of orthogonal THz polarization response in 2016. The switching of MCX cantilevers controls the x polarization response, while MCY cantilevers provide selective resonance switching only for y polarization [5]. A metamaterial of electromagnetic band gap was incorporated to an antenna for frequency reconfigurability. The EBG consisted of two identical unit cells that provided multiple band gaps respectively, in 1.88 to 1.94, 2.25 to 2.44, 2.67 to 2.94, 3.52 to 3.54, and 5.04 to 5.70 GHz with different EBG configurations. Subsequently, the antenna was incorporated with EBG. The corresponding incorporated structure successfully achieved various reconfigurable frequencies in 1.60, 1.91, 2.41, 3.26, 2.87, 5.21, and 5.54 GHz. The antenna had the potential to be implemented for the Bluetooth, Wi-Fi, WiMAX, LTE, and cognitive radio applications [6]. Choi et al. demonstrated a wideband reconfigurable double negative MMs using a complementary split-ring resonator. The resonator was made of quad-rings and by tailoring the quad-rings with switches, re-configurability and isotropic nature was investigated [7]. A left handed biaxial metamaterial was reported that has 5.81 GHz wide bandwidth and applicable for C-, X- and Ku-band applications in 2017. The total dimensions of the designed structure were  $0.2\lambda \times 0.2\lambda \times 0.035\lambda$  and the effective medium ratio 5.0, negative index bandwidth from 3.27 to 6.55 GHz, and 7.0

to 12.81 GHz along the z-axis wave propagation [8]. An effective negative refractive index was exhibited for the dual band of a fishnet-like MMs at millimeter-wave frequencies. The dual-band NRI behavior was achieved by the diffraction order ( $\pm 1, \pm 1$ ) associated with the internal mode [9]. Li et al. proposed a reconfigurable MMs frequency selective surface (FSS), where FSS composed of ceramic resonators with different band stop. In addition, the FSS could switch between two consecutive stop bands in 3.55 to 4.60 GHz, and 4.54 to 4.94 GHz [10]. An optically controlled reconfigurable hybrid metamaterial waveguide in the terahertz regime with photosensitive semiconductor incorporated into the MMs structure was presented by Zaho et al. in 2016 [11]. Han et al. offered a reconfigurable metamaterial developed by surface micromachining technique on a low loss quartz substrate for a tunable terahertz filter and the switching performance of the MMs was 16.50 dB in 480 GHz [12]. A reconfigurable MMs terahertz filter based on graphene was shown, which structure was consisting of periodic metallic rings with gaps, where graphene stripes were located and the resonance of the structure can be altered a 40% (from 0.2 to 0.12 THz) [13].

In this paper, a new reconfigurable metamaterial has been discussed for 5G application, where the frequency range is from 30.0 to 54. GHz. For 5G application, 37.0 to 40.50 GHz, 45.50 to 47.0 GHz, and 47.20 to 50.20 GHz, which have allocations to the mobile service on a primary basis as well as 31.80 to 33.40 GHz, and 40.50 to 42.50 GHz, which may require additional allocations to the mobile service on a primary basis. However, the proposed metamaterial show resonance peaks are respectively, 33.21, 39.89, 42.27, 45.86, and 48.41 GHz.

## 2. Structural design & methodology

The geometry of the proposed structure is designed by the resonator with splits and an I-shape inner metal bar is connected to the ring resonator, which is printed on an epoxy resin fibre (FR4) dielectric constant of  $\epsilon_r=4.6$ , loss tangent of  $\tan\delta=0.02$  and thickness of  $t=1.60$  mm used as a substrate material. FR-4 has a higher dissipation factor than most high frequency laminates. Typical dissipation factor values for FR-4 laminates increases steadily with frequency rises. The dimension of the metamaterial should be equal or less than  $(\lambda/4)$ . If the size of metamaterial is more than  $(\lambda/4)$  then the metamaterial might lose their significance. According to electromagnetic spectrum, for Ka-band the wavelength ( $\lambda$ ) of the metamaterial should be equal or less than 5 mm to 11.30 mm. Moreover, the proposed metamaterial wavelength ( $\lambda$ ) at 33.21 GHz is 9.09 mm. The schematic and equivalent lumped circuit of the proposed metamaterial is shown in Fig. 1(a-b). The specifications of the proposed reconfigurable metamaterial single unit cell are shown in Table 1.

Table 1. Specifications of the proposed reconfigurable metamaterial

Parameters Specification	Optimum Size (mm)
Length of the substrate material, A	30.0
Width of the substrate material, B	30.0
Length of the resonator, L	30.0
Width of the resonator, W	22.0
Width of the metal bar, d	4.0
Width of the gap, s	3.0

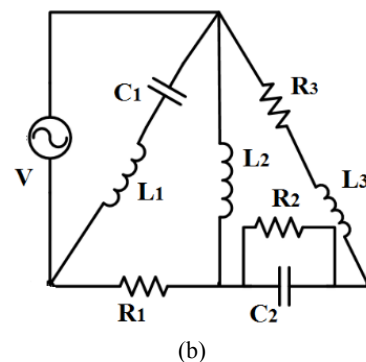
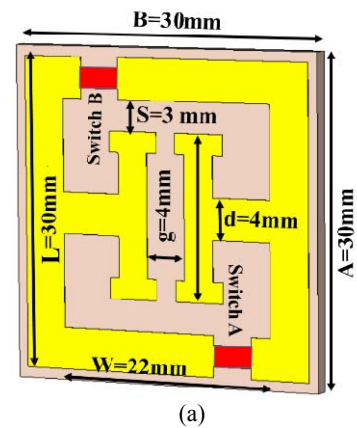


Fig. 1. Reconfigurable metamaterial single unit cell: (a) Schematic view, (b) Lumped elements equivalent circuit model at (both switch-A and switch-B open state)

From the equivalent lumped element circuit model of the metamaterial shown in Fig. 1(b), the inductance and capacitance are formed by the metal bar and slots, when the electromagnetic waves are incidence of the designed structure. With the raise of the inductance the resonance peaks shifted toward the lower frequency and the increase of the capacitance the resonance peaks move to the higher frequency [14]. Moreover,  $L_1$ ,  $L_2$ , and  $L_3$  are represented the inductance, whereas the capacitance is denoted by the  $C_1$ , and  $C_2$  in lumped equivalent circuit model. The simulated transmittance resonance at 33.21 GHz, whereas the calculated transmittance resonance at 33.05 GHz. The total calculated inductance and capacitance of the metamaterial structure at 33.05 GHz are 1.51 nH and 154.6 pF, respectively. The individual inductance are  $L_1$

(1.1 nH),  $L_2$  (2.7 nH) and  $L_3$  (4.3 nH) as well as capacitance are  $C_1$  (65.6 pF) and  $C_2$  (89 pF). Therefore, the resonance frequency is calculated by,

$$f_r = \frac{1}{2\pi\sqrt{L_T C_T}} \quad (1)$$

At different switching stage of the metamaterial the circuit model is almost similar but the effects of inductance and capacitance will be shifted. Because, the inductance are depend on the metallic resonator and strips of the structure as well as the capacitance are created by the splits in the resonator.

Recently, reconfigurable metamaterials (MMs) have attracted intense research interest since the active control of metamaterial performances. To design reconfigurable metamaterial, two switches (S-A and S-B) are placed on the resonator structure in between the splits as shown in Fig. 1(a). Depending on the state of switches, three different configurations (F-1, F-2, and F-3) are considered. The '0' and '1' states of switch are used for open and close conditions of switch, respectively. As described in table 2, configuration F-1 consists of both switches (S-A and S-B) are open. The F-2 configuration consists of switch S-A open and switch S-B close state as well as F-3 configuration consists of both switches (S-A and S-B) are close.

Table 2. State of the switch on different configuration

Configuration	State of Switch	
	S-A	S-B
F-1	0	0
F-2	0	1
F-3	1	1

The finite integration technique based electromagnetic simulator CST Microwave Studio is used to calculate the effective medium parameters [15]. The electromagnetic waves are propagated along the z-direction and perfect electric and magnetic boundaries are considered in the x- and y-direction for simulation from 30.0 to 54.0 GHz (Ka-band and Q-band) frequency range is shown in Fig. 2.

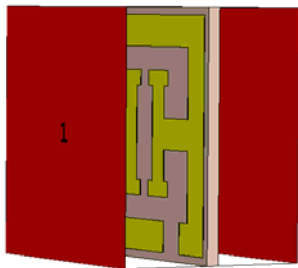
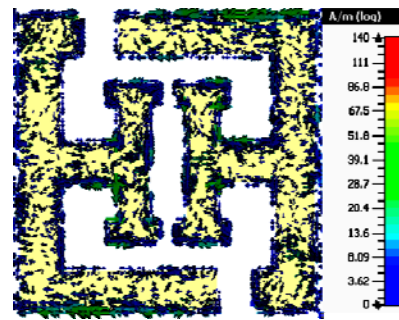


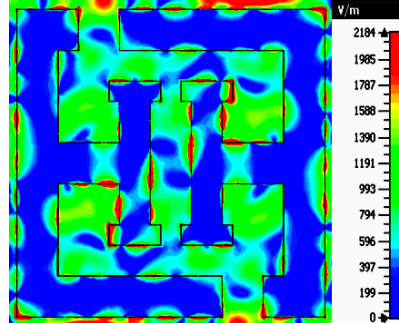
Fig. 2. Simulated geometry with boundary condition of the proposed reconfigurable metamaterial single unit cell at (switch-A open and switch-B open) state

### 3. Results and discussions

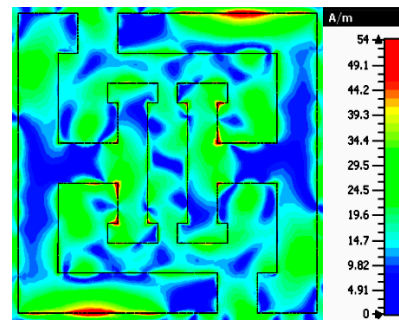
In the proposed structure the surface current is an electric current distribution that is created by the applied electromagnetic fields displayed in Fig. 3(a). The concentration of the current is more near and around the corner of the resonator. Due to the skin effect the intensity of the current is more on the outer resonator than the inner resonator. In addition, the opposite direction of the current is created for the dissimilar structure and slots of the proposed metamaterial. Further, the opposite direction current nullifies each other and causes the stop band. The electric and magnetic field distribution in 33.15 GHz is exhibited in Fig. 3(b-c).



(a)



(b)



(c)

Fig. 3. (a) Surface current, (b) Electric field, (c) Magnetic field, distribution at 33.21 GHz of the designed metamaterial at (switch-A open and switch-B open) state

When load is not perfectly matched to the transmission line, reflections at the load cause a negative traveling wave which causes unwanted standing wave in the transmission line. So, in case of transmission ( $S_{21}$ ) coefficients when it more negative amplitude at resonance points that means the load is perfectly matched and very little portion of the signal is reflected. In Fig. 4, the reflection ( $S_{11}$ ) and transmission ( $S_{21}$ ) coefficients for the proposed MMs are shown. The transmittance ( $S_{21}$ ) resonances are respectively, in 33.21 GHz (amplitude of -20.21 dB), 39.89 GHz (amplitude of -17.23 dB), 42.27 GHz (amplitude of -13.34 dB), 45.86 GHz (amplitude of -21.60 dB), and 48.41 GHz (amplitude of -25.64 dB) in figure 4. The reflection ( $S_{11}$ ) and transmission ( $S_{21}$ ) coefficients are vice versa. So, the proposed metamaterial structure is perfectly matched.

According to millimetre wave region are, 37.0 to 40.50 GHz, 42.50 to 43.50 GHz, 45.50 to 47.0 GHz, 47.20 to 50.20 GHz, which have allocations to the mobile service on a primary basis. Besides, 31.80 to 33.40 GHz, 40.50 to 42.50 GHz, and 47.0 to 47.20 GHz, which may require additional allocations to the mobile service on a primary basis for 5G wireless communications. As a result, from the above results analysis in the Fig. 4, the proposed metamaterial is applicable for 5G applications.

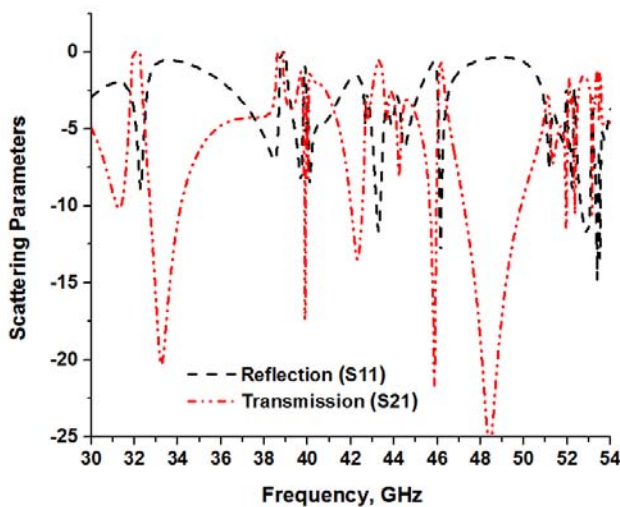


Fig. 4. Reflection ( $S_{11}$ ) and transmission ( $S_{21}$ ) coefficients of the designed metamaterial at (switch-A open and switch-B open) state

Fig. 5(a-c) demonstrates the effective medium parameters amplitude at different states of the (switch-A and switch-B) of the metamaterial. The amplitudes of the negative permittivity, permeability and refractive index are plotted, respectively in the same figure. From Fig. 5(a), the negative permittivity from 30.0 to 44.69 GHz, negative permeability from 35.11 to 36.69 GHz, 36.84 to 39.82 GHz, and 48.12 to 51.17 GHz, when the switch (S-A open and switch S-B open) state. Further, in figure 5(b) negative permittivity from 30.0 to 45.12 GHz, negative permeability from 35.18 to 41.0 GHz, 42.14 to 43.46 GHz, and 47.47 to 53.35 GHz, when the switch (S-A open and switch S-B close) state. As it is observed, there is a variation between the effective medium parameters (permittivity, permeability, and refractive index). Because when electromagnetic waves propagate through a material, its electric and magnetic fields oscillate in a sinusoidal pattern, and their velocity depends upon the material electrical conductivity, which in turn depends on the material internal structure. The relative speed of electrical signals traveling through a material varies according to how they interact with its internal structure. Therefore, variation in the internal structure of the metamaterial causes the variations in the effective medium parameters. Furthermore, for switch (S-A close and switch S-B close) state negative permittivity from 30.0 to 45.14 GHz and negative permeability from 35.14 to 38.74 GHz, 42.02 to 43.51 GHz, and 47.74 to 52.25 GHz in Fig. 5(c).

The extracted effective permittivity, permeability and refractive index are represent prove and characteristics of the metamaterial. According to the signs of permittivity ( $\epsilon$ ) and permeability ( $\mu$ ), when both permittivity and permeability are positive ( $\epsilon > 0$  and  $\mu > 0$ ), then it denotes as double positive material; when only permittivity is negative ( $\epsilon < 0$  and  $\mu > 0$ ) then it called Epsilon negative metamaterial; when only permeability is negative ( $\epsilon > 0$  and  $\mu < 0$ ) then it called Mu negative metamaterial; Finally, when both permittivity and permeability are negative ( $\epsilon < 0$  and  $\mu < 0$ ) then it called double negative metamaterial. From the Fig. 5(a-c), we observed the proposed metamaterial exhibits double negative characteristics in Fig. 5(a) at 36.8 GHz for Switch S-A open and switch S-B open state, in Fig. 5(b) at 38.3 GHz for Switch S-A open and switch S-B close state and in Fig. 5(c) at 36.8 GHz for Switch S-A close and switch S-B close state.

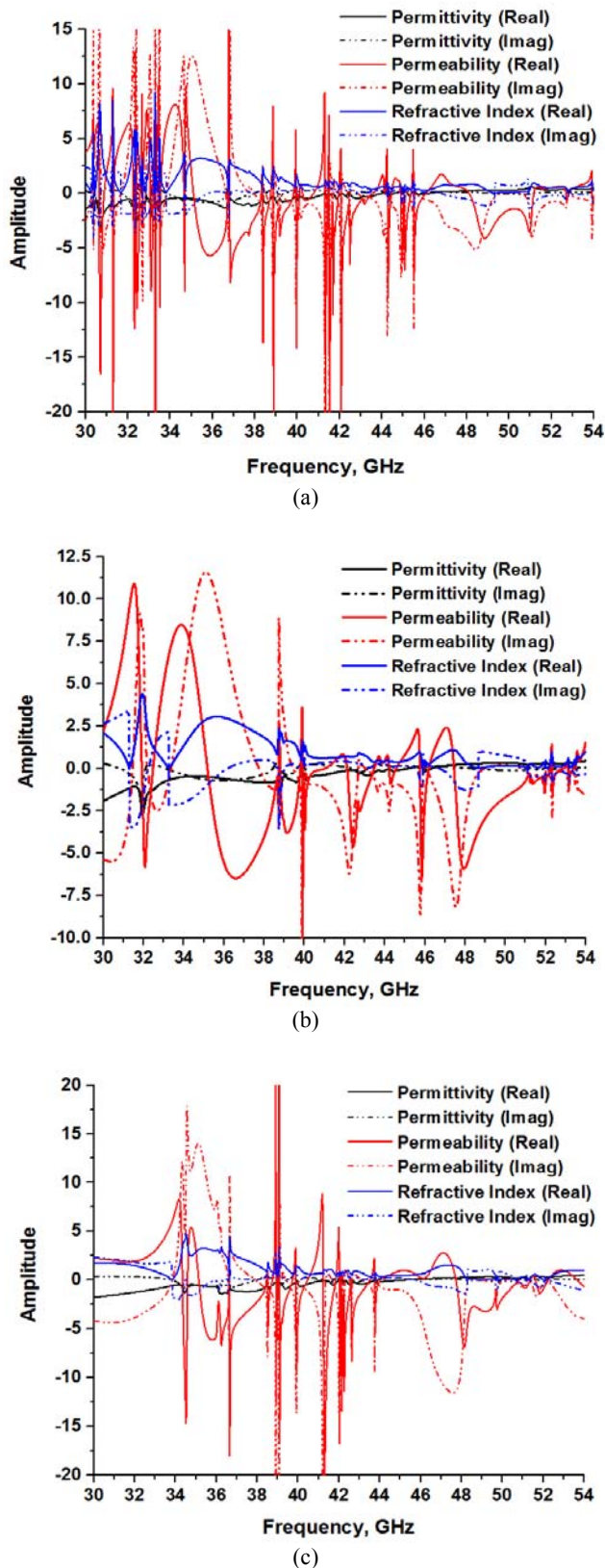


Fig. 5. Amplitude of the effective parameters ( $\epsilon$ ,  $\mu$  &  $n$ ), of the proposed reconfigurable metamaterial at different states of the switch: (a) Switch S-A open and switch S-B open state, (b) Switch S-A open and switch S-B close state, (c) Switch S-A close and switch S-B close state

#### 4. Conclusion

A reconfigurable metamaterial printed on FR-4 material has been proposed that resonances are in respectively, 33.21, 39.89, 42.27, 45.86, and 48.41 GHz in this paper. The electromagnetic waves are incident at z-direction and FIT-based CST electromagnetic simulator is used to obtain the reflection ( $S_{11}$ ) and transmission ( $S_{21}$ ) coefficients to calculate the effective medium parameters. The performance of the proposed metamaterial is also analyzed at different switching state. Finally, the designed reconfigurable metamaterial is flexible, compact, can cover wide bandwidth and applicable for 5G application.

#### Acknowledgements

This work was supported by the Research Universiti Grant, Geran Universiti Penyelidikan (GUP), Code: 2016-029.

#### References

- [1] D. R. Smith, W. J. Padilla, D. C. Vier, S. C. Nemat-Nasser, S. Schultz, *Physical Review Letters* **84**, 4184 (2000).
- [2] M. M. Hasan, M. R. I. Faruque, S. S. Islam, M. T. Islam, *Materials* **9**(10), 830 (2016).
- [3] S. S. Islam, M. M. Hasan, M. R. I. Faruque, M. M. Islam, M. T. Islam, *Microwave and Optical Technology Letters* **59**(5), 1092 (2017).
- [4] Y. H. Fu, A. Q. Liu, W. M. Zhu, X. M. Zhang, D. P. Tsai, J. B. Zhang, L. Chen, S. W. Qu, B. J. Chen, X. Bai, K. B. Ng, C. H. Chan, *Advance Functional Materials* **21**, 3589 (2011).
- [5] P. Pitchappa, C. P. Ho, L. Cong, R. Singh, N. Singh, C. Lee, *Advance Optical Mater* **4**, 391 (2016).
- [6] R. Dewan, M. K. A. Rahim, M. Himdi, M. R. Hamid, H. A. Majid, M. E. Jalil, *Applied Physics A* **123**(16), (2017).
- [7] J. H. Choi, C. W. Jung, *Microwave and Optical Technology Letters* **57**(11), (2015).
- [8] M. M. Hasan, M. R. I. Faruque, M. T. Islam, *Materials Research Express* **4**(3), (2017).
- [9] M. N. Cía, C. G. Meca, M. Beruete, A. Martínez, M. Sorolla, *Optics Letters* **36**(21), 4245 (2011).
- [10] L. Li, J. Wang, J. Wang, H. Ma, H. Du, J. Zhang, S. Qu, Z. Xu, *Scientific Reports* **6**, 24178 (2016).
- [11] X. Zhao, L. Zhu, C. Yuan, J. Yao, *Optics Express* **24**(16), 18244 (2016).
- [12] Z. Han, K. Kohno, H. Fujita, K. Hirakawa, H. Toshiyoshi, *Optics Express* **22**(18), 21326 (2014).
- [13] K. Yang, S. Liu, S. Arezoomandan, A. Nahata, B. S. Rodriguez, 8th International Congress on Advanced Electromagnetic Materials in Microwaves

- and Optics – Metamaterials, Denmark, 25-30 (2014).
- [14] M. M. Hasan, M. R. I. Faruque M. T. Islam, IEEE Access **5**, 21217 (2017).
- [15] M. M. Hasan, M. R. I. Faruque, M. T. Islam, Microwave and Optical Technology Letters **59(6)**, 1450 (2017).

---

\*Corresponding author: mehedi20.kuet@gmail.com,  
rashed@ukm.edu.my